AM-Align: Globally Optimal Estimation of Accelerometer-Magnetometer Misalignment

Xiangcheng Hu, Jin Wu, Bohuan Xue, Yilong Zhu, Mingkai Jia, Yuhua Qi, Yi Jiang, Ping Tan and Wei Zhang

***Abstract*—Construction robots require accurate sensing of their own localization information for precision perception, actuation and control. The calibration of the accelerometer-magnetometer combination is a vital step to guarantee accuracy for estimating position and attitude. Previously, the misalignment (extrinsic) calibration between the accelerometer and magnetometer has been significantly studied. However, these algorithms require sufficient and outlier-free data to guarantee a satisfactory initial guess for further optimization. In this paper, a novel globally optimal method, AM-Align, is developed to solve this problem. The proposed method is independent of an initial guess and robust in insufficient data and outliers. To achieve this goal, all global optima are sought by finding the solution set with the least loss function values using the polynomial eigenvalue method. Simulation studies show the complete solution set of the minimal case of the studied problem. Experimental results verify the superiority of the proposed scheme against previous representative candidates, showing that AM-Align requires fewer measurements and has higher accuracy together with good robustness.**

***Index Terms*—Accelerometer, magnetometer, sensor alignment, sensor calibration, attitude estimation**

I. Introduction

BUILDING up highly accurate integrated navigation system is of great significance in construction robots. Accelerometers and magnetometers are crucial components in modern sensor systems, providing cost-effective solutions for attitude estimation in various applications, such as robotics, aviation, and automotive systems [1]. These sensors enable accurate navigation in complex environments by leveraging accelerometer readings for tilt angles and magnetometer data for heading relative to the Earth's magnetic north. The widespread adoption of micro-electro-mechanical-system (MEMS) technology has made these sensors small, low-cost, and flexible. However, the accuracy of MEMS sensors depends heavily on proper calibration. Arising from misalignment errors during sensor integration, the accelerometer-magnetometer alignment (AMA) problem has been extensively studied in recent years. While traditional approaches often rely on costly equipment, making them impractical for field applications and consumer-level products. Zhang et al. [2] propose a quaternion-based Kalman filter with vector selection for accurate orientation tracking, considering sensor misalignment and calibration parameters. Vasconcelos et al. [3] present a geometric approach for strapdown magnetometer calibration in the sensor frame, estimating the misalignment between the magnetometer and inertial sensor axes. Wu and Shi [4] introduce a calibration method for three-axis magnetometers that estimates sensor biases, scale factors, and non-orthogonality using a maximum likelihood estimator. Sotiriadis et al. [5], [6] address the problem of orientation sensor fusion and calibration for motion tracking in mobile devices, proposing a fusion algorithm that combines data from accelerometers, gyroscopes, and magnetometers while considering their misalignment and calibration parameters. Despite the progress made in accelerometer-magnetometer alignment, several challenges and limitations persist:

- **Initialization dependency**: Many existing alignment methods rely on a good initial guess of the transformation between the accelerometer and magnetometer frames, which can lead to suboptimal solutions or divergence if poorly initialized.
- **Robustness to noise and outliers**: Magnetometer data, susceptible to environmental magnetic disturbances, require robust calibration and alignment to mitigate noise and outliers.
- **Computational complexity**: AMA algorithms demand intensive computations, including optimization and matrix operations, challenging their implementation on devices with limited computational resources.

This paper focuses on addressing these limitations by emphasizing:

1) We propose a globally optimal method for solving the accelerometer-magnetometer alignment problem, independent of initial guess and robust to insufficient and outlier-corrupted data.
2) By exploiting the algebraic structure of the sensor measurement models, we formulate the alignment problem as a constrained least-squares optimization in unit quaternion space. This problem is further reduced to a system of multivariate polynomial equations, which is solved efficiently using the polynomial eigenvalue technique.

II. Problems and Solution

For a vector-field sensor, the raw readings can be modeled as follows $\boldsymbol{v}^{\mathrm{b}} = \boldsymbol{S}\boldsymbol{R}\boldsymbol{v}^{\mathrm{r}} + \boldsymbol{b}_{\boldsymbol{v}} + \boldsymbol{\epsilon}_{\boldsymbol{v}}$, where $\boldsymbol{v}^{\mathrm{b}}$ and $\boldsymbol{v}^{\mathrm{b}}$ are 3-D vector measurements in the body frame and reference frame respectively; $\boldsymbol{S} \in \mathbb{R}^{3\times3}$ stands for the calibration matrix that takes scale factor and nonorthogonality into account; $\boldsymbol{R}$ is the rotation matrix in the special orthogonal group $\mathrm{SO}(3) := \left\{\boldsymbol{R} \in \mathbb{R}^{3\times3} \,\middle|\, \boldsymbol{R}^{\top}\boldsymbol{R} = \boldsymbol{I}, \det(\boldsymbol{R}) = 1\right\}$; $\boldsymbol{b}_{\boldsymbol{v}}$ and $\boldsymbol{\epsilon}_{\boldsymbol{v}} \sim \mathcal{N}(\boldsymbol{0}, \boldsymbol{\Sigma}_{\boldsymbol{v}})$ denote the constant bias and stochastic noise term respectively. The noise covariance matrix can typically be modeled as isotropic one $\boldsymbol{\Sigma}_{\boldsymbol{v}} = \gamma^2\boldsymbol{I}$ in which γ stands for the variance or noise level. In this paper, r-frame is the North-East-Down (NED) reference frame. The *intrinsic* calibration problem of vector-field sensor is to estimate unknown parameters $\boldsymbol{S}, \boldsymbol{R}, \boldsymbol{b}_{\boldsymbol{v}}$ and sometimes, $\boldsymbol{v}^{\mathrm{r}}$, with given measurements of $\boldsymbol{v}^{\mathrm{b}}$. For accelerometer, $\boldsymbol{v}^{\mathrm{r}}$ is known and can be set to $\boldsymbol{v}^{\mathrm{r}} = (0, 0, 9.8)^{\top}\ \mathrm{m/s^2}$ in the NED frame. For magnetometer, however, since $\boldsymbol{v}^{\mathrm{r}}$ is the function of local geodetic coordinates, $\boldsymbol{v}^{\mathrm{r}}$ should be estimated as well. Intrinsic calibration of magnetometers has been extensively studied. Thus, the practitioners can employ methods e.g. [4], [7], [8] for *ad-hoc* calibration prior to a specific use. Misaliangment estimation is detailed in the following.

A. Proposed Misalignment Calibration

After a proper intrinsic calibration procedure, the accelerometer and magnetometer in the non-distorted condition have the following measurements related by the rotation matrix $\boldsymbol{R} \in \mathrm{SO}(3)$:

$$\boldsymbol{a}^{\mathrm{b}} = \boldsymbol{R}\boldsymbol{a}^{\mathrm{r}}, \quad \boldsymbol{m}^{\mathrm{b}} = \boldsymbol{R}\boldsymbol{m}^{\mathrm{r}} \tag{1}$$

X. Hu and J. Wu contributed equally to the contents of this paper.

X. Hu, J. Wu, B. Xue, Y. Zhu, M. Jia, P. Tan, W. Zhang are with the Department of Electronic and Computer Engineering, Hong Kong University of Science and Technology, Hong Kong, China (E-mail: xhubd@connect.ust.hk).

Y. Qi is currently with School of Systems Science and Engineering, Sun Yat-Sen University, Guangzhou, China (E-mail: qiyh8@mail.sysu.edu.cn)

Y. Jiang is with the Department of Electrical Engineering, City University of Hong Kong, Hong Kong, China (E-mail: yjian22@cityu.edu.hk).

in which $\boldsymbol{a}^{\mathrm{b}}$ and $\boldsymbol{m}^{\mathrm{b}}$ are **normalized** measurements in the body frame from the accelerometer and magnetometer respectively; $\boldsymbol{a}^{\mathrm{r}} = (0,0,1)^{\top}$ and $\boldsymbol{m}^{\mathrm{r}} = (m_{\mathrm{N}},0,m_{\mathrm{D}})^{\top}$ denote the corresponding normalized vectors in the NED frame while m_{N} and m_{D} are components in the North and Down directions, respectively. A fact in these sensor models is that

$$\boldsymbol{a}^{\mathrm{b}} \cdot \boldsymbol{m}^{\mathrm{b}} = (\boldsymbol{a}^{\mathrm{r}})\, \boldsymbol{R}^{\top} \boldsymbol{R} \boldsymbol{m}^{\mathrm{r}} = \boldsymbol{a}^{\mathrm{r}} \cdot \boldsymbol{m}^{\mathrm{r}} \tag{2}$$

which is the dot-product equality for attitude determination from two vector observations, which has been extensively adopted in calibration and attitude determination [9]–[11]. Expanding (2) gives

$$\boldsymbol{a}^{\mathrm{b}} \cdot \boldsymbol{m}^{\mathrm{b}} = \|\boldsymbol{a}^{\mathrm{r}}\| \, \|\boldsymbol{m}^{\mathrm{r}}\| \cos\theta = \cos\theta \tag{3}$$

where θ is the local magnetic dip angle. For common accelerometer-magnetometer combinations, the alignment between the two sensors may not be refined. Therefore, when using the two sensors for attitude estimation, the frame misalignment between them must be determined. Denoting the rotation from magnetometer to accelerometer as $\boldsymbol{R}^{\mathrm{a}}_{\mathrm{m}}$, it is able to relate the measured normalized magnetic field $\tilde{\boldsymbol{m}}^{\mathrm{b}}$ in magnetometer frame and corresponding $\boldsymbol{m}^{\mathrm{b}}$ in the accelerometer frame by $\boldsymbol{m}^{\mathrm{b}} = \boldsymbol{R}^{\mathrm{a}}_{\mathrm{m}} \tilde{\boldsymbol{m}}^{\mathrm{b}}$. Therefore (3) becomes

$$\boldsymbol{a}^{\mathrm{b}} \cdot \boldsymbol{m}^{\mathrm{b}} = \left(\boldsymbol{a}^{\mathrm{b}}\right)^{\top} \boldsymbol{R}^{\mathrm{a}}_{\mathrm{m}} \tilde{\boldsymbol{m}}^{\mathrm{b}} = \cos\theta \tag{4}$$

From (4), one can observe that there are two unknowns i.e. $\boldsymbol{R}^{\mathrm{a}}_{\mathrm{m}}$ and θ. Thus the task of the accelerometer-magnetometer alignment is to estimate $\boldsymbol{R}^{\mathrm{a}}_{\mathrm{m}}$ and θ from multiple-position measurements of $\boldsymbol{a}^{\mathrm{b}}$ and $\boldsymbol{m}^{\mathrm{b}}$ in a simultaneous manner. The kernel optimization is expressed as follows

$$\underset{\boldsymbol{R}^{\mathrm{a}}_{\mathrm{m}} \in \mathrm{SO}(3), \theta \in \mathbb{R}}{\arg\min} \; \mathcal{L} = \sum_{i \in \mathcal{I}} \left[\left(\boldsymbol{a}^{\mathrm{b}}_{i}\right)^{\top} \boldsymbol{R}^{\mathrm{a}}_{\mathrm{m}} \tilde{\boldsymbol{m}}^{\mathrm{b}}_{i} - \cos\theta \right]^2 \tag{5}$$

in which i denotes the sample index of accelerometer and magnetometer measurements while $\mathcal{I}$ indicates all indices of available inliers. Optimization (5) can be interpreted as

$$\underset{\boldsymbol{R}^{\mathrm{a}}_{\mathrm{m}} \in \mathrm{SO}(3), s \in \mathbb{R}}{\arg\min} \; \mathcal{L} = \sum_{i \in \mathcal{I}} \left[\left(\boldsymbol{a}^{\mathrm{b}}_{i}\right)^{\top} \boldsymbol{R}^{\mathrm{a}}_{\mathrm{m}} \tilde{\boldsymbol{m}}^{\mathrm{b}}_{i} - s \right]^2, \quad \text{s.t. } |s| \leq 1 \tag{6}$$

where $s = \cos\theta$. In [5], an analytical algorithm is designed to compute closed-form approximation of $\boldsymbol{R}^{\mathrm{a}}_{\mathrm{m}}$ and s from (6). Then gradient-descent algorithm is applied to solve a refined solution from the closed-form initial guess. The method in [5] is practical and accurate but can only be feasible in the condition that a matrix $\boldsymbol{A}$ stacked in rows by $\tilde{\boldsymbol{m}}^{\mathrm{b}}_{i} \otimes \boldsymbol{a}^{\mathrm{b}}_{i}$ for $i \in \mathcal{I}$ is of full rank. If $\boldsymbol{A}$ is rank-deficient, the estimated approximation of $\mathrm{vec}\,(\boldsymbol{R}^{\mathrm{a}}_{\mathrm{m}})$ will not be a proper initial guess and may diverge to a local minimum in a further gradient-descent search. To guarantee the rank of $\boldsymbol{A}$, at least 9 different pairs of measurements are required. However, from (6), one can conclude that $\boldsymbol{R}^{\mathrm{a}}_{\mathrm{m}}$ and s are observable in the condition that there are at least four pairs of measurements. This is because the rotation matrix $\boldsymbol{R}^{\mathrm{a}}_{\mathrm{m}}$ has three degrees of freedom. This paper solves the problem (6) without a closed-form initial guess, but rather by using the Gröbner-basis method, the global optimum can be sought with high accuracy. Choosing $\boldsymbol{q}^{\mathrm{a}}_{\mathrm{m}}$ as the quaternion of $\boldsymbol{R}^{\mathrm{a}}_{\mathrm{m}}$, it is able for us to write the gradient of $\mathcal{L}$ as $\nabla_{\boldsymbol{y}} \mathcal{L} = \frac{\partial \mathcal{L}}{\partial \boldsymbol{y}}$, where $\boldsymbol{y} = \left[(\boldsymbol{q}^{\mathrm{a}}_{\mathrm{m}})^{\top}, s \right]^{\top}$. All local minima and maxima occur in the condition of $\nabla_{\boldsymbol{y}} \mathcal{L} = \boldsymbol{0}$. By extending $\nabla_{\boldsymbol{y}} \mathcal{L} = \boldsymbol{0}$, one obtains

$$s = \frac{1}{\mathcal{N}} \sum_{i \in \mathcal{I}} \left(\boldsymbol{a}^{\mathrm{b}}_{i}\right)^{\top} \boldsymbol{R}^{\mathrm{a}}_{\mathrm{m}} \tilde{\boldsymbol{m}}^{\mathrm{b}}_{i} \tag{7}$$

Inserting (7) into the original objective $\mathcal{L}$ gives a new optimization objective $\hat{\mathcal{L}}$ without s, say $\arg\min_{\|\boldsymbol{q}^{\mathrm{a}}_{\mathrm{m}}\|=1} \hat{\mathcal{L}}\,(\boldsymbol{q}^{\mathrm{a}}_{\mathrm{m}})$. The optimization can be solved by constructing the Lagrangian, such that $\tilde{\mathcal{L}} = \hat{\mathcal{L}} + \lambda \left[(\boldsymbol{q}^{\mathrm{a}}_{\mathrm{m}})^{\top} \boldsymbol{q}^{\mathrm{a}}_{\mathrm{m}} - 1 \right]$, where λ is the Lagrange multiplier. The quaternion and Lagrange multiplier can be sought by means of

$$\nabla_{\boldsymbol{\zeta}} \tilde{\mathcal{L}} = \boldsymbol{0} \tag{8}$$

where $\boldsymbol{\zeta} = \left[(\boldsymbol{q}^{\mathrm{a}}_{\mathrm{m}})^{\top}, \lambda \right]^{\top}$. This will construct a polynomial system of 5 sub-equations. Each equation has different sets of monomials. The first 4 sub-equations are essential for the solution of $\boldsymbol{q}^{\mathrm{a}}_{\mathrm{m}}$. And the rest is simply the quaternion unit norm condition. If we parameterize quaternion as $\boldsymbol{q}^{\mathrm{a}}_{\mathrm{m}} = (q_0, q_1, q_2, q_3)^{\top}$, the first 4 sets of monomials can be summarized as quadratic 21 monomials of q_0, q_1, q_2, q_3 and λ. The coefficients rely on input measurements, whose analytical forms can be given by symbolic engines of mathematical software like Python `SymPy` or Mathworks `MATLAB`. From these monomials, we can see that they have common parts, but are not the same for the rest parts. All these monomials form a cubic polynomial system to be solved. To obtain all local minima of $\boldsymbol{q}^{\mathrm{a}}_{\mathrm{m}}$, one needs to solve all solutions of $\boldsymbol{q}^{\mathrm{a}}_{\mathrm{m}}$ and λ. This indicates that we are dealing with a 5-variable cubic polynomial system. There is no closed-form solution to such a high-order polynomial system, according to the Abel-Ruffini theorem [12]. However, by using Bezout's theorem [13], we can obtain the maximum solution count of this system, i.e., it has at most $5 \times 4^{(}3 - 1) = 80$ distinct solutions. Although according to Bezout's theorem, we have concluded that our system to be solved has at most 80 distinct solutions, since one quaternion and its negative represent the same rotation, there are at most 40 solutions to be found. Note that not all these 40 solutions are in the real space. Therefore, only real solutions will be considered, which normally covers $4 \sim 16$ real solutions in engineering practice. After all real local quaternion critical points are obtained, inserting them back into (7) gives multiple $s = \cos\theta$. Then, inserting these quaternions along with s critical points back into the original objective function $\mathcal{L}$ produces a number array, with which we obtain the globally optimal solution corresponding to the least objective function value after a typical sort algorithm. We use the polynomial eigenvalue solution to solve all possible solutions for this system [14]. The polynomial eigenvalue method is a rigorous mathematical approach for solving systems of polynomial equations of the form $f(\boldsymbol{x}) = \boldsymbol{0}$, where f is a polynomial function and $\boldsymbol{x}$ is an unknown vector. The generalized eigenvalue problem associated with the polynomial system $f(\boldsymbol{x}) = \boldsymbol{0}$ is given by $\boldsymbol{H}\boldsymbol{\varrho} = \mu \boldsymbol{G}\boldsymbol{\varrho}$, where $\mu \in \mathcal{K}$ is an eigenvalue and $\boldsymbol{\varrho} \in \mathcal{K}^k$ is a corresponding eigenvector. The solutions to the polynomial system can be obtained from the eigenvectors $\boldsymbol{\varrho}$ by considering the appropriate components that correspond to the original variables $\boldsymbol{x}$. In this work, we use MATLAB `mupad` symbolic engine to derive the symbolic manipulation of constructing matrices $\boldsymbol{H}$ and $\boldsymbol{G}$. Specifically, we use `equationsToMatrix` function to extract coefficients for $\boldsymbol{H}$ and $\boldsymbol{G}$. All the coefficient extraction works are conducted offline. Thus, the actual execution speed of the algorithm is fast in practice. Finally, the QZ algorithm in `Eigen` library is used for C++ implementation.

III. Experimental Results

A. Numerical Example: Minimal Case

When we have $\mathcal{N} \geq 4$ pairs of accelerometer-magnetometer measurements, the polynomial system in (8) becomes solvable. Fig. 1 shows a minimal configuration of sensor placements. However, when exactly $\mathcal{N} = 4$, which is the minimal case of the studied problem, it can be empirically obtained that there are at most 6 ambiguous optimal solutions of a total of 40 distinct ones simultaneously satisfying the polynomial system. Sometimes, the minimal system has 4 ambiguous optimal solutions, which depend on the parameter configuration. We call this phenomenon the mirror effect of the solutions. If $\mathcal{N} = 5$, the 5-th pair of measurements helps with

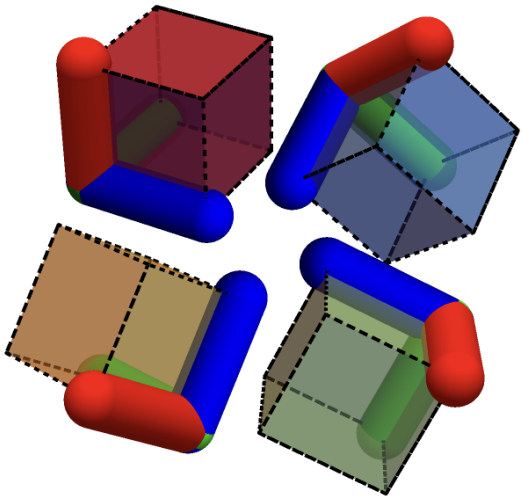

Fig. 1: The minimal sensor placements required for AM-Align. The red, green, and blue axes denote the Euler angles in roll, pitch, and yaw, respectively. Only 4 different poses are needed for a complete calibration, which is less than that in existing representatives.

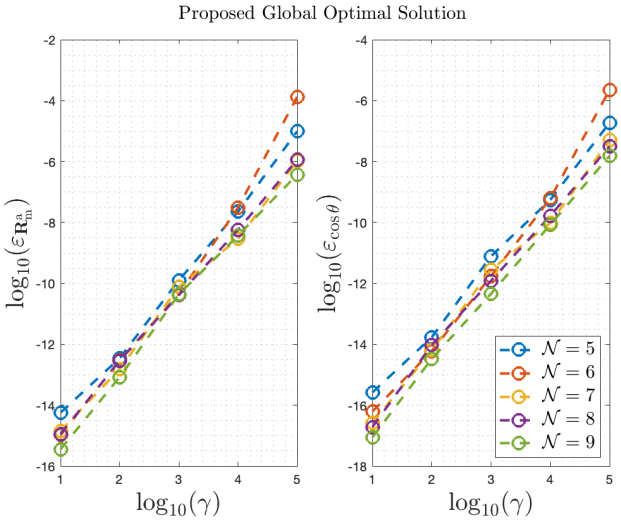

Fig. 2: The error statistics of AM-Align with increasing $\mathcal{N}$. All cases are convergent.

verifying which of the ambiguous solutions is correct. To be clear, we present here a numerical example showing how the system is solved in the minimal case. We simulate the true misalignment rotation as $\boldsymbol{R}^{\mathrm{a}}_{\mathrm{m,true}}$ with $\cos\theta_{\mathrm{true}} = 0.861311153421915$, which denotes a position in the Northern hemisphere. The normalized accelerometer and magnetometer measurement pairs are simulated using model (1) with the noise level of $\gamma = 10^{-3}$ for accelerometer with a unit of $\mathrm{m/sec}^2$ and for magnetometer with a unit of Gauss, as $\boldsymbol{a}^{\mathrm{b}}_1, \boldsymbol{a}^{\mathrm{b}}_2, \boldsymbol{a}^{\mathrm{b}}_3, \boldsymbol{a}^{\mathrm{b}}_4, \boldsymbol{m}^{\mathrm{b}}_1, \boldsymbol{m}^{\mathrm{b}}_2, \boldsymbol{m}^{\mathrm{b}}_3, \boldsymbol{m}^{\mathrm{b}}_4$. with which we construct the optimization kernel and is later solved using AM-Align. The proposed algorithm returns 6 pairs of distinct real solutions, see `https://github.com/JokerJohn/AM_Align/blob/main/suppl.pdf`. It can be seen from the results that the 2-nd pair of solutions $\boldsymbol{R}^{\mathrm{a}}_{\mathrm{m},2}$ is the correct one. Commonly, the correct solution can also be deduced via the $\cos\theta$ value according to the local geodetic position.

Multiple Monte-Carlo simulations are performed with different numbers of measurements for AM-Align and the existing method

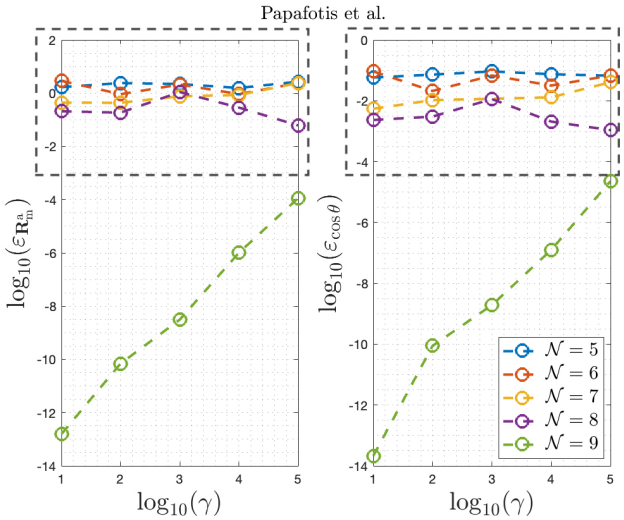

Fig. 3: The error statistics of the method by Papafotis et al. with increasing $\mathcal{N}$. The dashed boxes denote the divergent estimates when $\mathcal{N} < 9$.

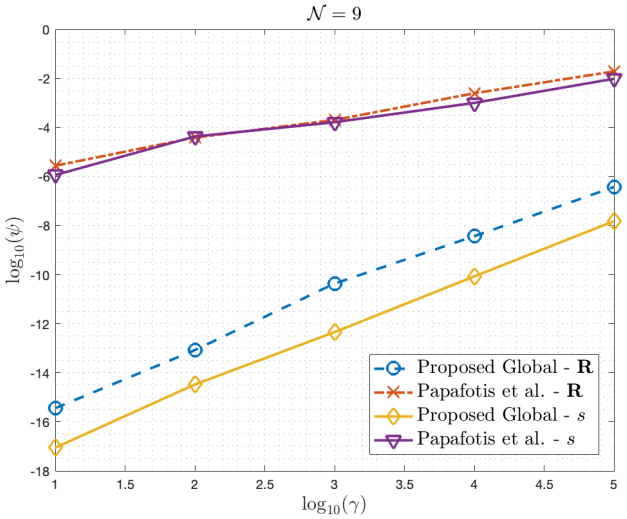

Fig. 4: The error statistics of various algorithms when $\mathcal{N} = 9$, in which ψ denotes the error metrics of either $\varepsilon_{\boldsymbol{R}^{\mathrm{a}}_{\mathrm{m}}}$ or $\varepsilon_{\cos\theta}$. Still, AM-Align has better estimation accuracy.

[15]. We simulate over 10000 samples for each case with different $\mathcal{N}$ and noise levels γ and get mean results. The error metrics are $\varepsilon_{\boldsymbol{R}^{\mathrm{a}}_{\mathrm{m}}} = \arccos\ \frac{1}{2}\mathrm{tr}(\boldsymbol{R}^{\mathrm{a}}_{\mathrm{m}}\boldsymbol{R}^{\top}_{\mathrm{true}}) - 1$ and $\varepsilon_{\cos\theta} = |\cos\theta - \cos\theta_{\mathrm{true}}|$.

The results are shown in Fig. 2 and 3 respectively. The results indicate that AM-Align requires less numbers of measurements. We also inspect the error results of various candidates when $\mathcal{N} = 9$, which are depicted in Fig. 4. The results also indicate that the proposed method, according to its globally optimal nature, has better estimation accuracy than the compared representative.

B. Hardware Synthesis

AM-Align is implemented on an unmanned aerial vehicle platform where the inertial measurement unit and magnetometer are synchronized using hardware clocks and impulses. We first perform an intrinsic calibration task for the magnetometer using the Riemannian method proposed recently [16], guaranteeing that all external magnetic-field distortions and disturbances are eliminated. After that, AM-Align is used for misalignment calibration. We compare the dot product $\left(\boldsymbol{a}^{\mathrm{b}}\right)^{\top}\boldsymbol{m}^{\mathrm{b}}$ before and after the calibration (see Fig. 6). The

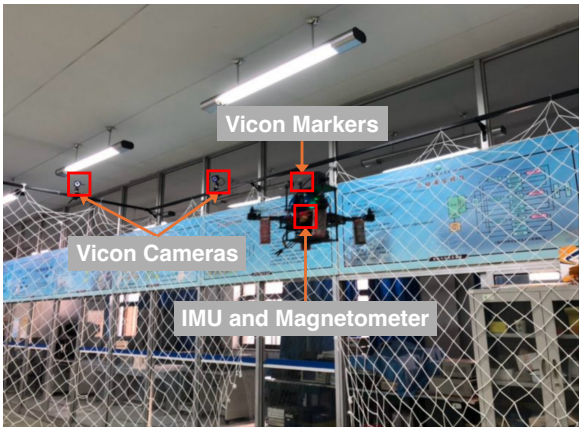

Fig. 5: The unmanned aerial vehicle platform used for hardware synthesis and verification. The platform is tested in a laboratory with Vicon motion-capture ground-truth system.

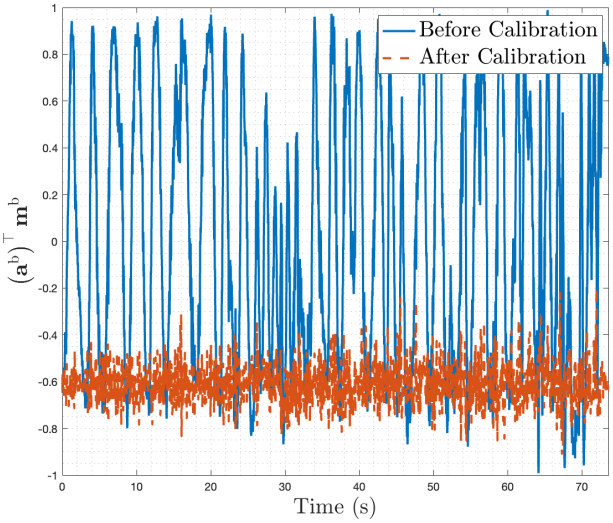

Fig. 6: The $\left(\boldsymbol{a}^{\mathrm{b}}\right)^{\top}\boldsymbol{m}^{\mathrm{b}}$ values before and after the calibration using the proposed globally optimal method.

results indicate that AM-Align is effective with the in-field robot as it significantly increases the consistency of $\left(\boldsymbol{a}^{\mathrm{b}}\right)^{\top}\boldsymbol{m}^{\mathrm{b}}$, which is the kernel metric for evaluation of the calibration.

Fig. 7: The employed construction robot cooperated with Transforma Robotics, PTE, Ltd., Singapore, for validation of state estimation accuracy using AM-Align calibrated accelerometer and magnetometer.

The proposed AM-align method has been deployed on a construction robot product that we cooperated with Transforma Robotics, PTE, Ltd., Singapore, as shown in Fig. 7. In prototyping stage, We employ the renowned ECL library for robot state estimation in PX4 autonomous systems[1], which consists usage of IMU and magnetometer as sensor inputs. We compare the attitude accuracy with the ground truth device MTi-G-710 that is rigidly attached to the body of the robot. The results show that the attitude error of the robot has been lowered from an average of 2.755 deg to 1.603 deg, which verifies the efficacy of the proposed method.

IV. Conclusion

This paper presented a globally optimal method for estimating the misalignment between an accelerometer and a magnetometer. The proposed AM-Align formulates the alignment problem as a constrained least-squares optimization in unit quaternion space, which is reduced to a system of multivariate polynomial equations and solved efficiently using the polynomial eigenvalue technique. Experiments demonstrate that our algorithm outperforms state-of-the-art methods in terms of accuracy and robustness under various conditions. Future works include developing simultaneous intrinsic and extrinsic calibration for accelerometer and magnetometer via minimum trajectory configuration of sensor motion.

References

[1] D. Von Arx, C. Fischer, H. Torlakcik, S. Pane, B. J. Nelson, and Q. Boehler, "Simultaneous Localization and Actuation Using Electromagnetic Navigation Systems," *IEEE Trans. Robot.*, vol. 40, pp. 1292–1308, 2024.

[2] Z.-q. Zhang and G.-z. Yang, "Micromagnetometer Calibration for Accurate Orientation Estimation," *IEEE Trans. Biomed. Eng.*, vol. 62, no. 2, pp. 553–560, 2015.

[3] J. F. Vasconcelos, G. Elkaim, C. Silvestre, P. Oliveira, and B. Cardeira, "Geometric approach to strapdown magnetometer calibration in sensor frame," *IEEE Trans. Aerosp. Elect. Syst.*, vol. 47, no. 2, pp. 1293–1306, 2011.

[4] Y. Wu and W. Shi, "On Calibration of Three-Axis Magnetometer," *IEEE Sensors J.*, vol. 15, no. 11, pp. 6424–6431, 2015.

[5] P. P. Sotiriadis and K. Papafotis, "A Single-Step Method for Accelerometer and Magnetometer Axes Alignment," *IEEE Trans. Instrum. Meas.*, vol. 9456, no. c, pp. 1–1, 2020.

[6] ——, "Accurate Analytical Accelerometer-Magnetometer Axes Alignment Guaranteeing Exact Orthogonality," *IEEE Trans. Instrum. Meas.*, vol. 70, 2021.

[7] Z. Wu, Y. Wu, X. Hu, and M. Wu, "Calibration of three-axis magnetometer using stretching particle swarm optimization algorithm," *IEEE Trans. Instrum. Meas.*, vol. 62, no. 2, pp. 281–292, 2013.

[8] Z. Q. Zhang and G. Z. Yang, "Calibration of miniature inertial and magnetic sensor units for robust attitude estimation," *IEEE Trans. Instrum. Meas.*, vol. 63, no. 3, pp. 711–718, 2014.

[9] X. Li and Z. Li, "Vector-aided in-field calibration method for low-end MEMS gyros in attitude and heading reference systems," *IEEE Trans. Instrum. Meas.*, vol. 63, no. 11, pp. 2675–2681, 2014.

[10] L. Jie, Z. Xiaoming, L. Jun, and C. Guobin, "Calibration of triaxial MEMS vector field measurement system," *IET Sci. Meas. Tech.*, vol. 8, no. 6, pp. 601–609, 2014.

[11] J. Wu, Z. Zhou, H. Fourati, and Y. Cheng, "A Super Fast Attitude Determination Algorithm for Consumer-Level Accelerometer and Magnetometer," *IEEE Trans. Consumer Elect.*, vol. 64, no. 3, pp. 375–381, 2018.

[12] P. Ramond, "The abel–ruffini theorem: Complex but not complicated," *American Math. Monthly*, vol. 129, no. 3, pp. 231–245, 2022.

[13] M. Shub and S. Smale, "Complexity of bézout's theorem. i. geometric aspects," *J. American Math. Society*, vol. 6, no. 2, pp. 459–501, 1993.

[14] Z. Kukelova, M. Bujnak, and T. Pajdla, "Polynomial eigenvalue solutions to minimal problems in computer vision," *IEEE Trans. Pattern Anal. Mach. Intell.*, vol. 34, no. 7, pp. 1381–1393, 2012.

[15] K. Papafotis and P. P. Sotiriadis, "MAG.I.C.AL.-A Unified Methodology for Magnetic and Inertial Sensors Calibration and Alignment," *IEEE Sensors J.*, vol. 19, no. 18, pp. 8241–8251, 2019.

[16] J. Cheng, M. Jia, B. Xue, and J. Wu, "Field Vector Sensor Calibration Using Riemannian Optimization Techniques on the Oblique Manifold," *IEEE Trans. Instrum. Meas.*, 2024.

[1] https://github.com/PX4/PX4-ECL